# Supporting Information

## Coordination compounds based on a phosphonic amide-TEMPO diradical and $Cu^{II}$, $Nd^{III}$, $Eu^{III}$ and $Tb^{III}$ ions: synthesis, magnetic properties and application in the aerobic oxidation of allylic and benzylic alcohols

Yolanda Navarro,[a] Stéphane Soriano,[c] Henrique de Castro Silva Jr.,[b,d] María José Iglesias,[a] Guilherme P. Guedes*[b] and Fernando López Ortiz*[a]

[a]*Área de Química Orgánica, Centro de Investigación CIAIMBITAL, Universidad de Almería, Carretera de Sacramento s/n, 04120 Almería, Spain. E-mail: flortiz@ual.es*

[b]*Universidade Federal Fluminense, Instituto de Química, Departamento de Química Inorgânica, Niterói, Rio de Janeiro, Brazil E-mail: guilherme_guedes@id.uff.br*

[c]*Instituto de Física, Universidade Federal Fluminense, Niterói-RJ, Brazil.*

[d]*Universidade Federal Rural do Rio de Janeiro, Instituto de Química, Departamento de Química Fundamental, Seropédica, Rio de Janeiro, Brazil.*

**Contents**

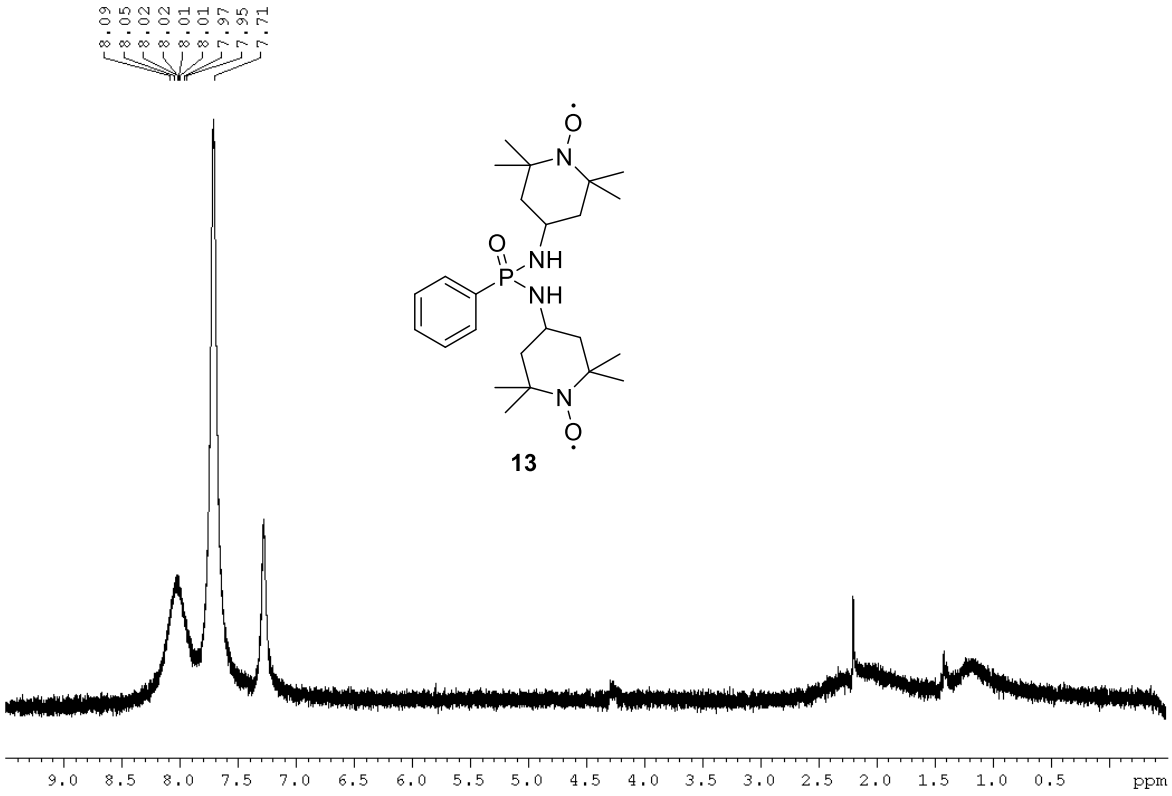


**Fig. S1.** $^{1}$H NMR spectrum ($CDCl_3$, 300.13 MHz) of **13**.

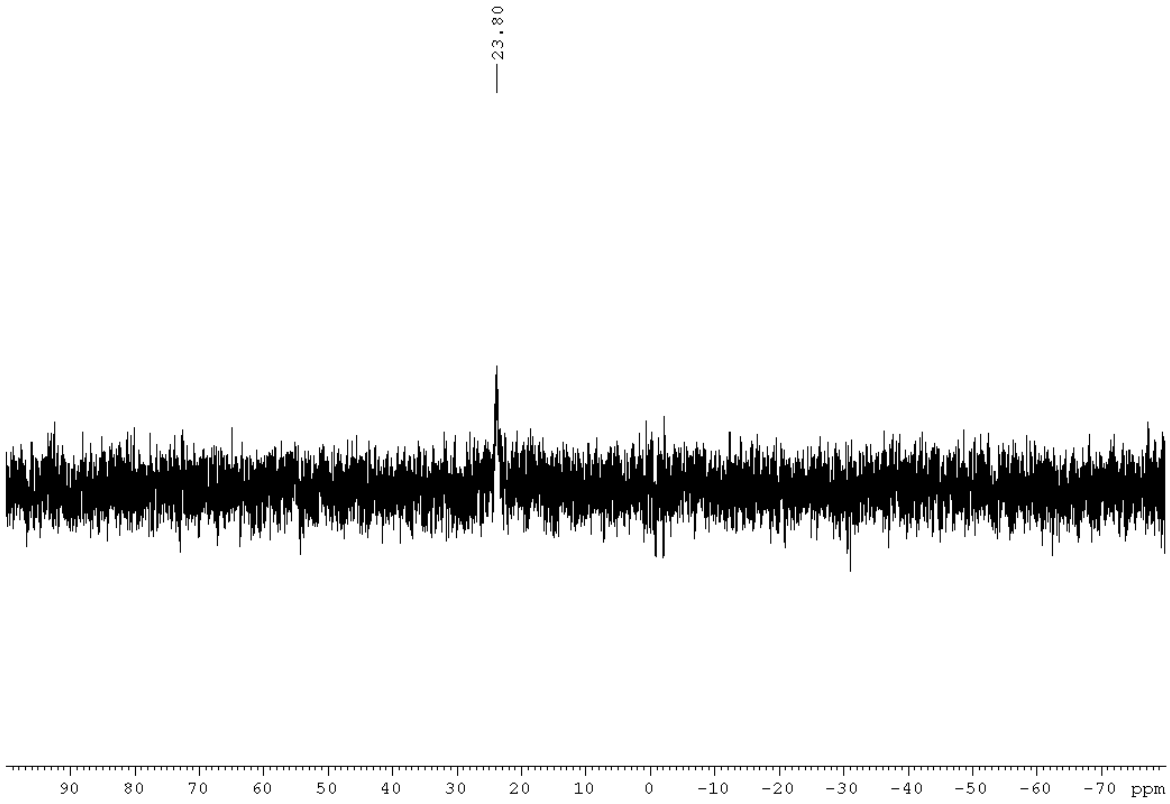


**Fig. S2.** $^{31}$P NMR spectrum ($CDCl_3$, 121.50 MHz) of **13**.

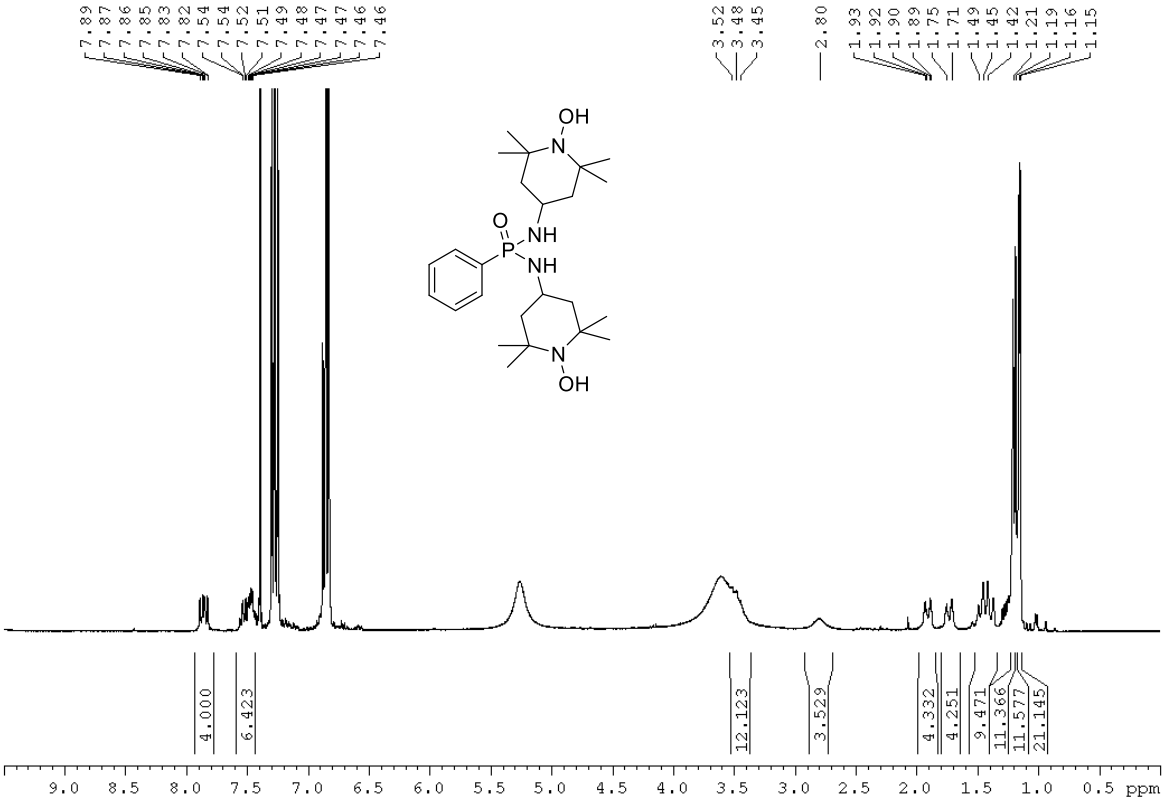


**Fig. S3.** $^{1}$H NMR spectrum ($CDCl_3$, 300.13 MHz) of **13** in the presence of phenylhydrazine.

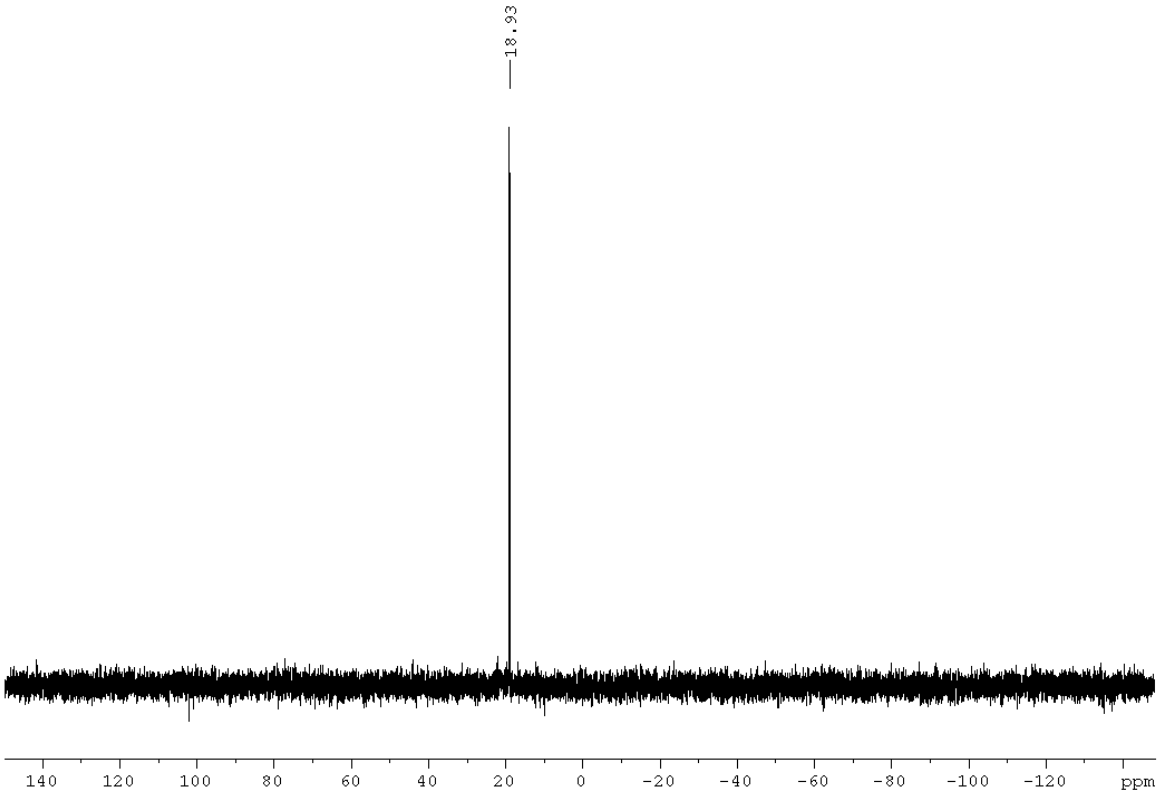


**Fig. S4.** $^{31}$P NMR spectrum ($CDCl_3$, 121.50 MHz) of **13** in the presence of phenylhydrazine.

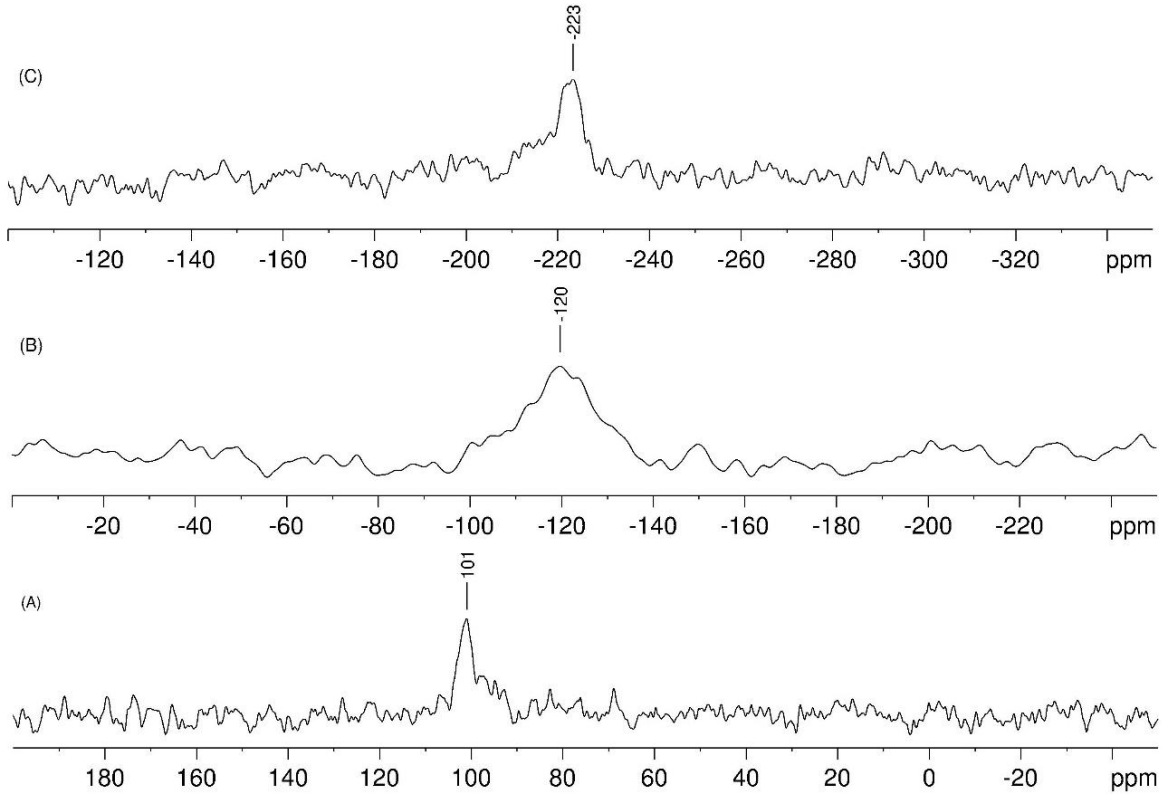


**Fig. S5.** $^{31}$P NMR spectra (121.50 MHz) of **15** in $CDCl_3$ (A), **16** in $CD_3CN$ (B) and **17** in $CDCl_3$ (C). In all cases, the FID was multiplied by an exponential function prior to the Fourier transformation. The line broadening parameters used were LB = 100 for **15** and **17** and LB = 400 for **16**.

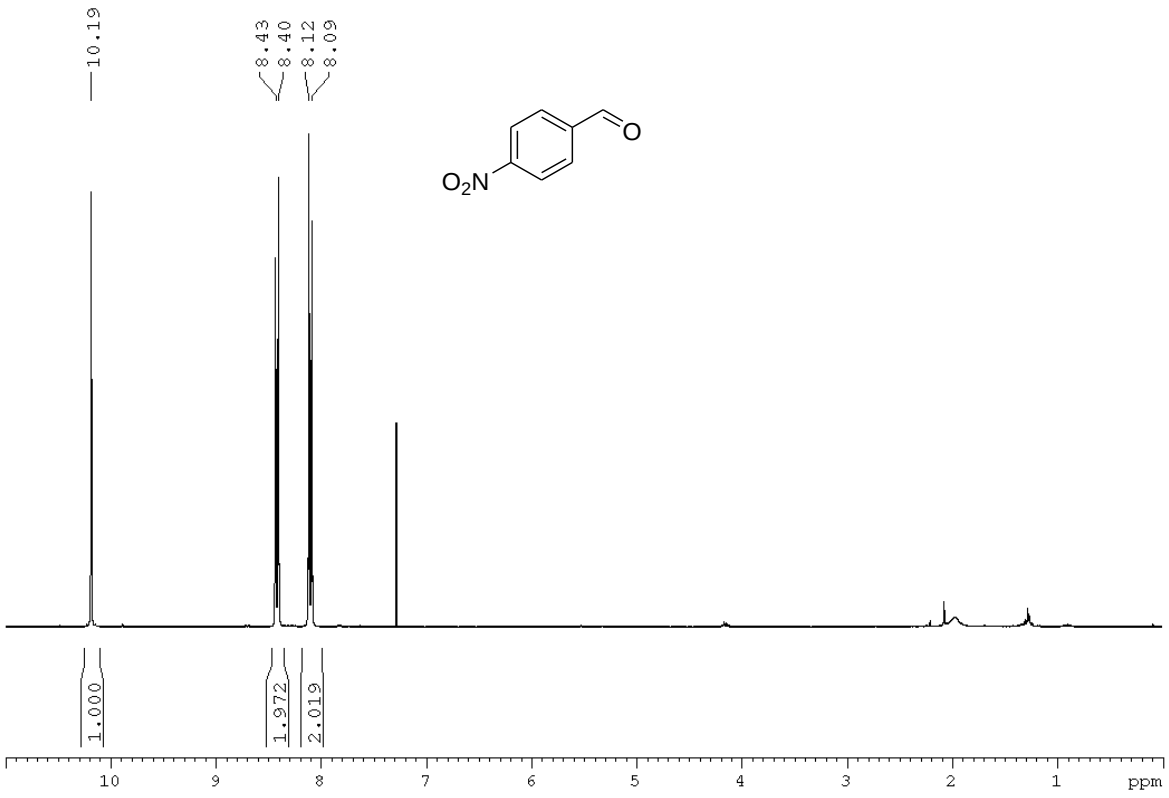


**Fig. S6.** $^{1}$H NMR spectrum ($CDCl_3$, 300.13 MHz) of **19**.

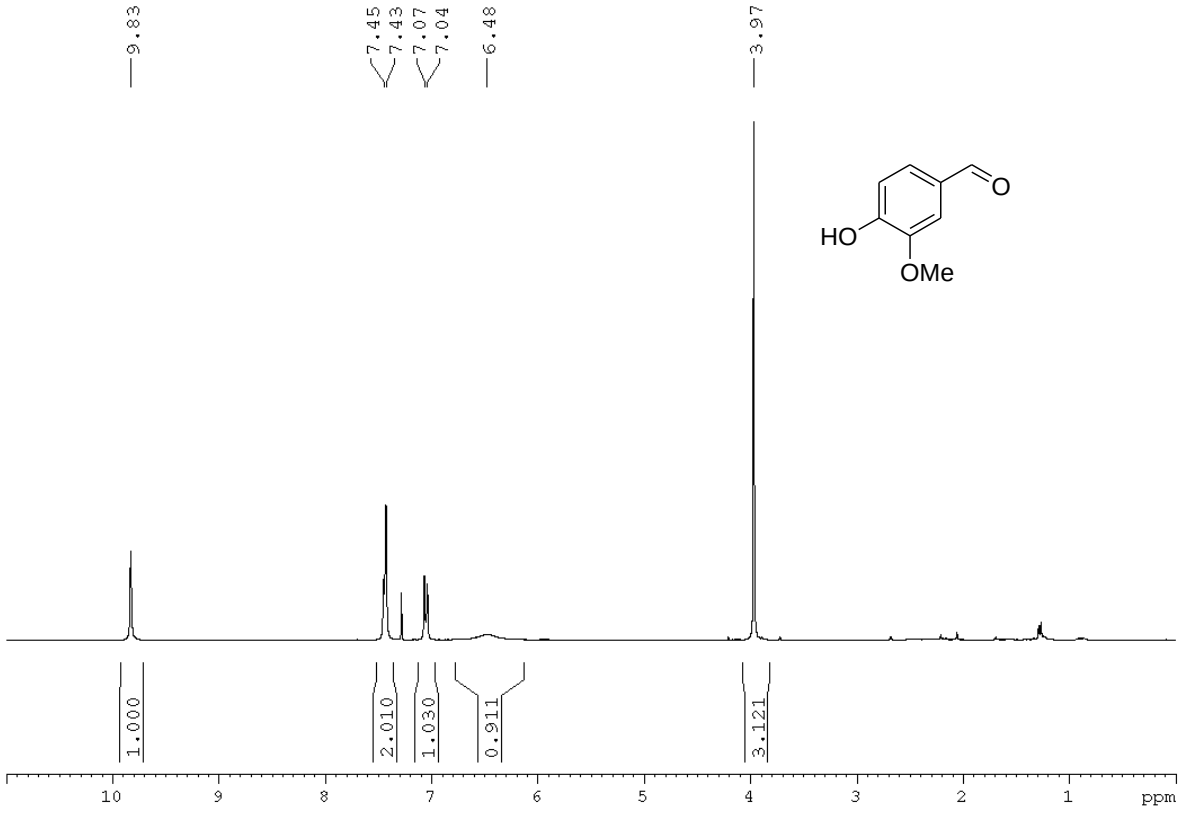


**Fig. S7.** $^{1}$H NMR spectrum ($CDCl_3$, 300.13 MHz) of **22**.

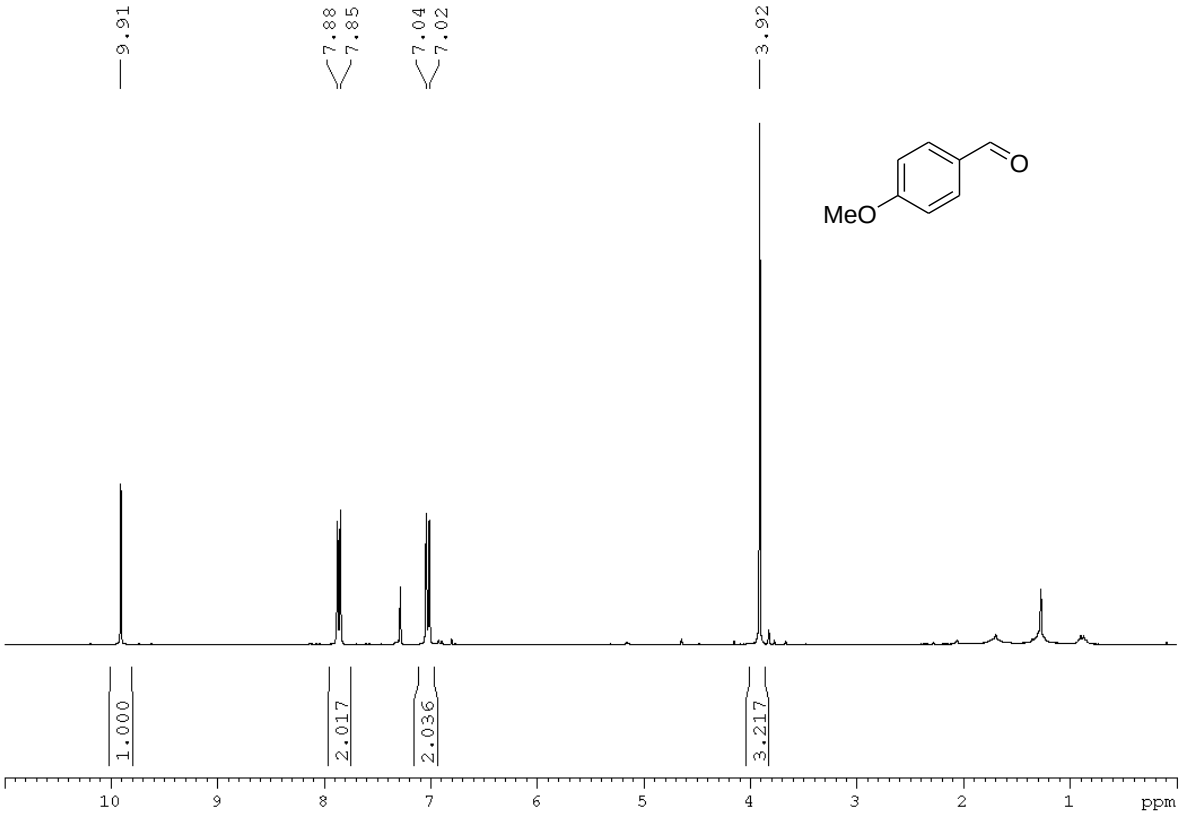


**Fig. S8.** $^{1}$H NMR spectrum ($CDCl_3$, 300.13 MHz) of **23**.

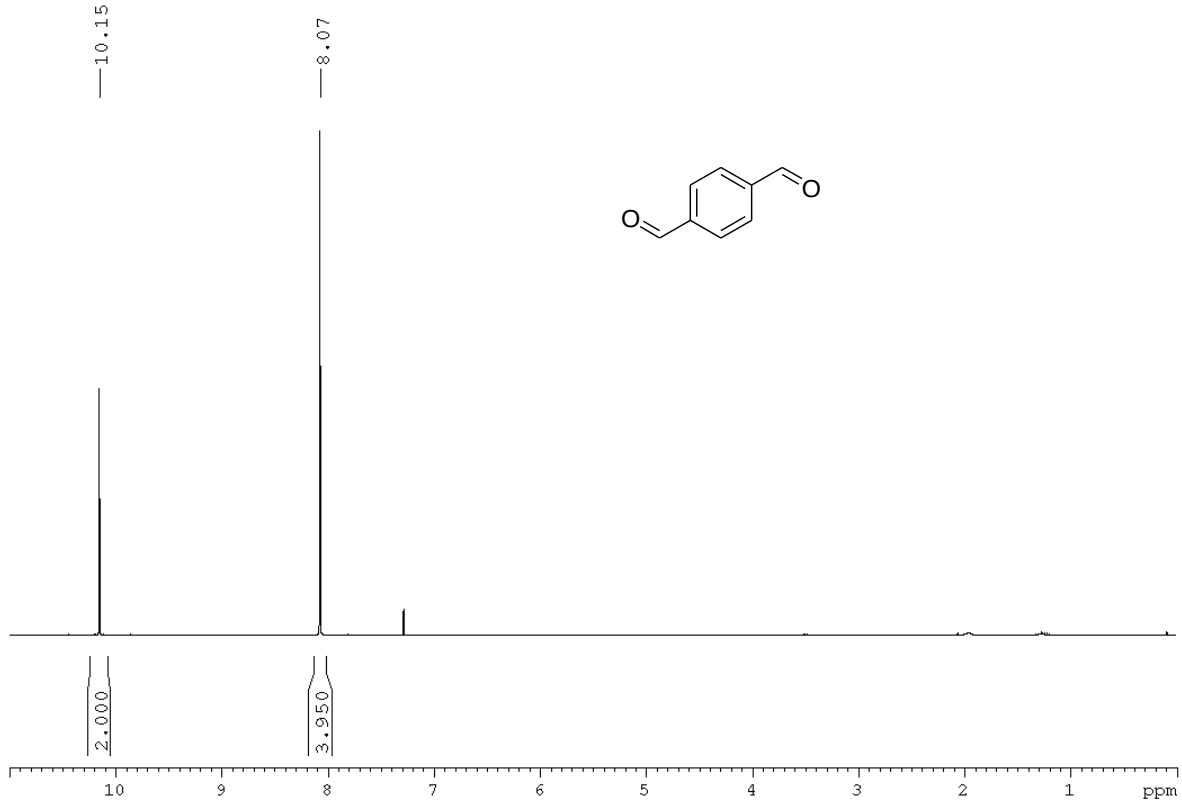


**Fig. S9.** $^{1}$H NMR spectrum ($CDCl_3$, 300.13 MHz) of **26**.

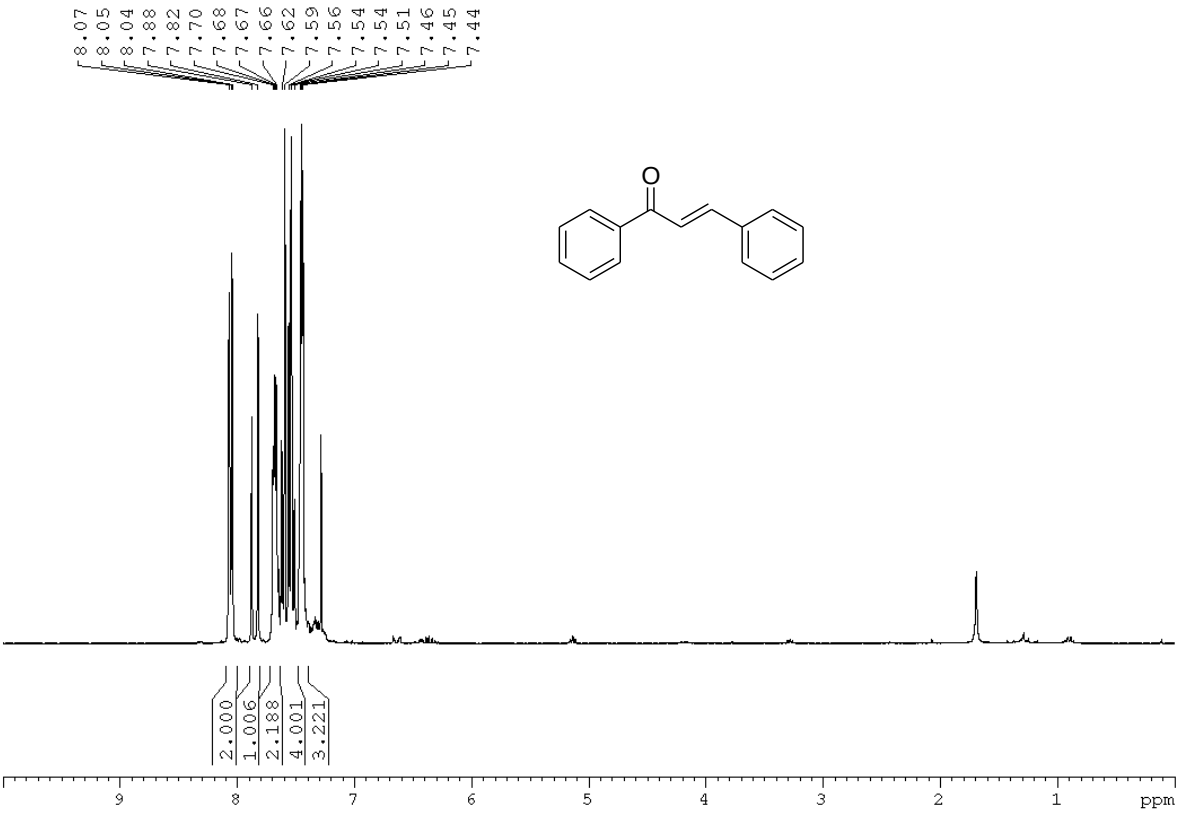


**Fig. S10.** $^{1}$H NMR spectrum ($CDCl_3$, 300.13 MHz) of **29**.

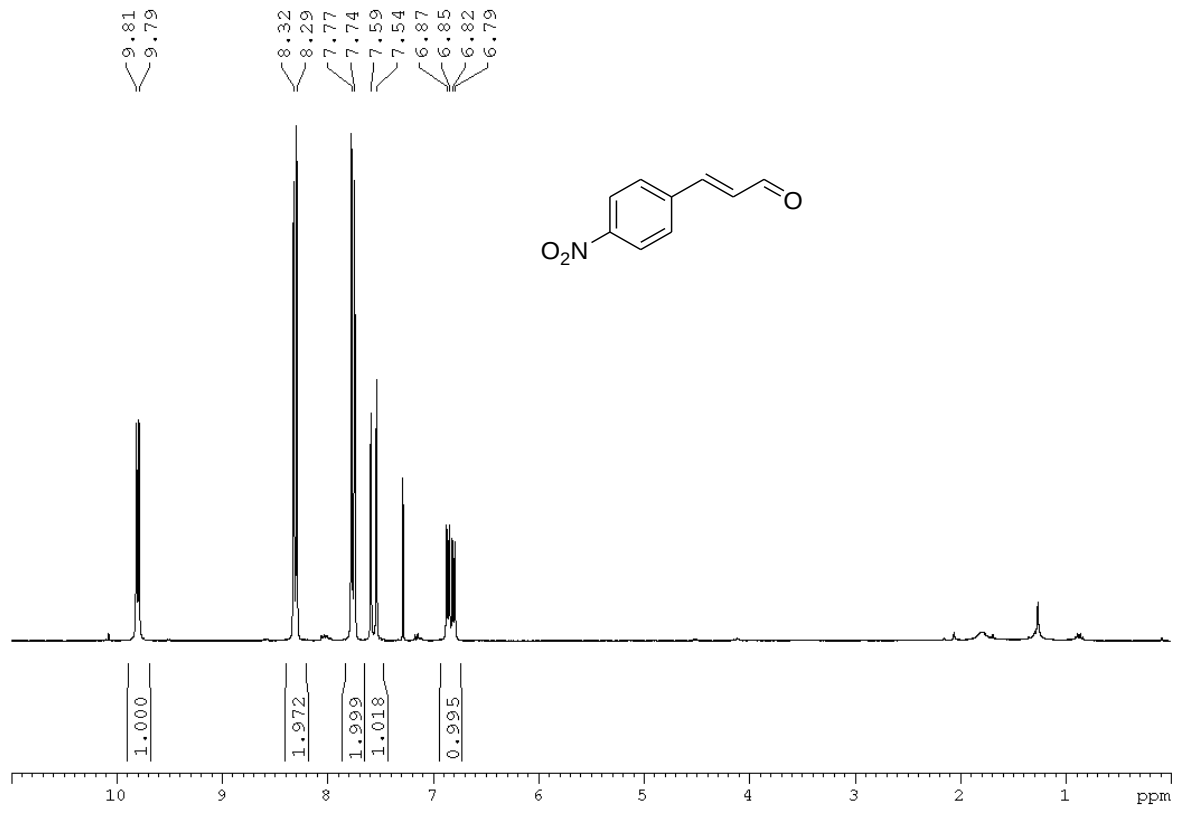


**Fig. S11.** $^{1}$H NMR spectrum ($CDCl_3$, 300.13 MHz) of **32**.

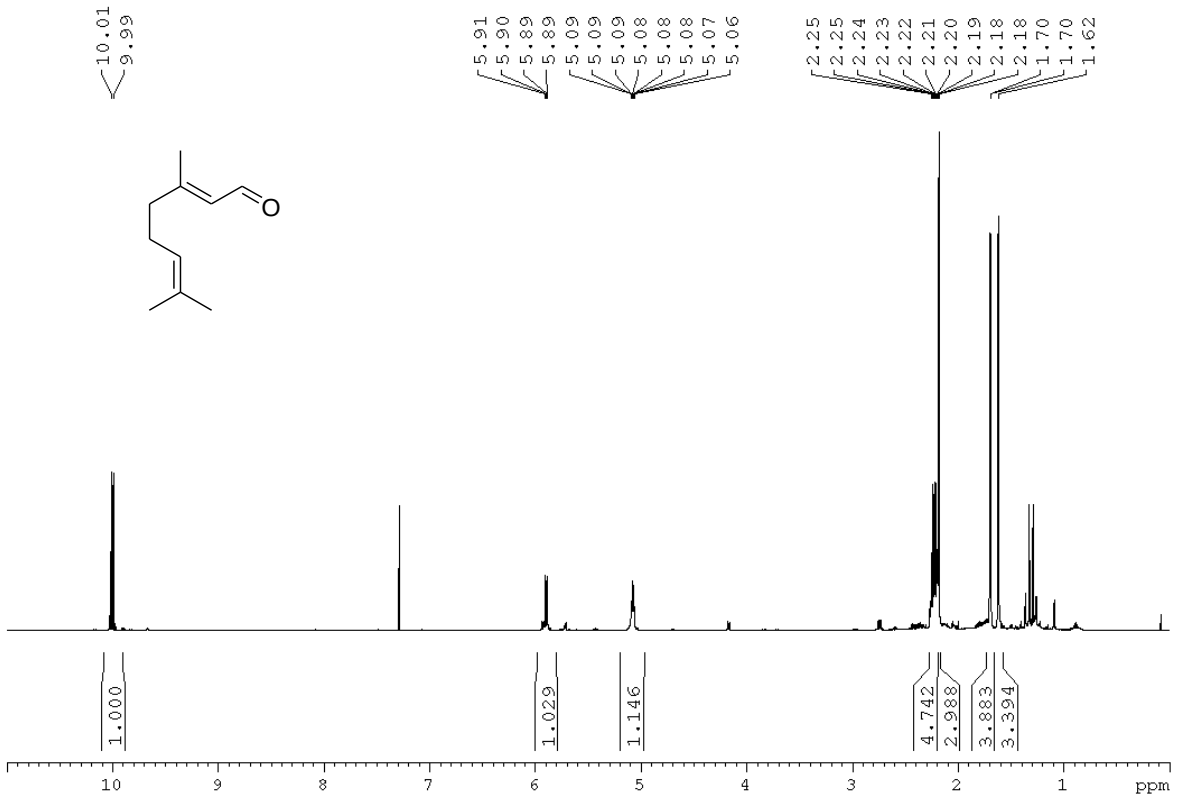


**Fig. S12.** $^{1}$H NMR spectrum ($CDCl_3$, 300.13 MHz) of **33**.

**Model used to fit the magnetic properties of compound 16 at high temperature**

Considering the long distances between radicals or between radical and metal ion within the molecule in the crystal structure, we didn´t take into account any magnetic interaction between the magnetic species at high temperature. Therefore, the DC magnetic susceptibility was modeled as the sum of the individual contributions of the four radicals and of the $Eu^{3+}$ ion.

$$\chi = 4\chi_{rad} + \chi_{Eu}$$

With respect to the $Eu^{3+}$ ion, the $^7F$ ground term is split by the spin-orbit coupling into seven states $^7F_J$, with their energy increasing with J.

$$E(J) = \lambda J(J+1)/2$$

where λ is the spin-orbit coupling parameter. Taking into account all seven spin-orbit coupled states, the magnetic susceptibility can be calculated by the following equation:[1]

$$\chi_{Eu} = \frac{\mu_B^2}{3\lambda}\ \frac{C}{D}$$

with

$$C = 24 + (27x/2 - 3/2)e^{-x} + (135x/2 - 5/2)e^{-3x} + (189x - 7/2)e^{-6x} + (405x - 9/2)e^{-10x} + (1485x/2 - 11/2)e^{-15x} + (2457x/2 - 13/2)e^{-21x}$$

$$D = 1 + 3e^{-x} + 5e^{-3x} + 7e^{-6x} + 9e^{-10x} + 11e^{-15x} + 13e^{-21x}$$

and $x = \lambda/k_BT$

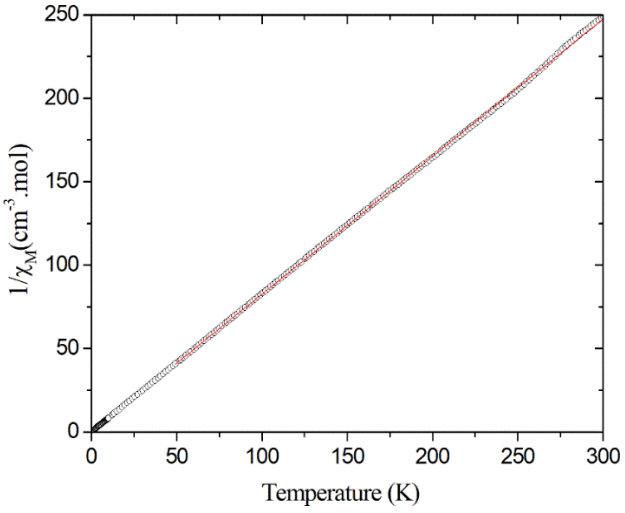


**Fig. S13**. Temperature dependence of the reciprocal of susceptibility for compound **14**.

**Table S1:** Summary of the crystal structure, data collection and refinement parameters for **13**-**17**.

| **Compound reference** | **13** | **14** | **15** | **16** | **17** |
|---|---|---|---|---|---|
| Chemical formula | $C_{24}H_{41}N_4O_3P$ | $C_{41}H_{51}CuF_{12}N_4O_7P$ | $C_{63}H_{85}F_{18}N_8NdO_{12}P_2$ | $C_{63}H_{85}EuF_{18}N_8O_{12}P_2$ | $C_{63}H_{85}F_{18}N_8O_{12}P_2Tb$ |
| Formula Mass /g.mol$^{-1}$ | 464.58 | 1034.38 | 1694.56 | 1702.28 | 1709.27 |
| Crystal system | Monoclinic | Monoclinic | Orthorhombic | Orthorhombic | Monoclinic |
| Space group | $P2_1/n$ | C2/c | A*ba*2 | A*ba*2 | $P2_1/n$ |
| *a*/Å | 13.7016(3) | 38.926(2) | 19.4450(5) | 19.5128(4) | 12.2774(3) |
| *b*/Å | 10.0092(3) | 12.0395(6) | 23.4941(4) | 23.4721(5) | 31.7772(6) |
| *c*/Å | 19.0510(5) | 20.668(1) | 17.649(4) | 17.5090(5) | 20.0260(4) |
| $\alpha$/° | 90 | 90 | 90 | 90 | 90 |
| $\beta$/° | 95.077(1) | 111.217(4) | 90 | 90 | 95.2292(11) |
| $\gamma$/° | 90 | 90 | 90 | 90 | 90 |
| Unit cell volume/Å$^3$ | 2602.44(12) | 9029.4(8) | 8059.1(3) | 8019.2(3) | 7780.5(3) |
| *Z* | 4 | 8 | 4 | 4 | 4 |
| Temperature/K | 100 | 100 | 100 | 100 | 100 |
| Radiation type | CuK$\alpha$ | CuK$\alpha$ | CuK$\alpha$ | MoK$\alpha$ | CuK$\alpha$ |
| $\mu$/mm$^{-1}$ | 1.18 | 1.88 | 6.17 | 0.92 | 5.77 |
| Measured reflections | 113365 | 192100 | 99067 | 148932 | 54954 |
| Independent reflections | 5140 | 8908 | 7635 | 12229 | 12794 |
| $R_{int}$ | 0.055 | 0.077 | 0.069 | 0.082 | 0.049 |
| $R_1$ ($F^2>2\sigma(F^2)$) | 0.037 | 0.060 | 0.040 | 0.032 | 0.039 |
| $wR(F^2)$ | 0.084 | 0.142 | 0.095 | 0.062 | 0.081 |
| $R_1$ (all data) | 0.045 | 0.078 | 0.048 | 0.042 | 0.051 |
| $wR(F^2)$ (all data) | 0.088 | 0.152 | 0.100 | 0.066 | 0.086 |
| Goodness of fit on $F^2$ | 1.04 | 1.03 | 1.05 | 1.05 | 1.02 |
| CCDC Deposition | 2501504 | 2501505 | 2501506 | 2501507 | 2501508 |

For **13**: $w = 1/[\sigma^2(F_o^2) + (0.0324P)^2 + 1.8766P]$; For **14**: $w = 1/[\sigma^2(F_o^2) + (0.0566P)^2 + 50.4372P]$; For **15**: $w = 1/[\sigma^2(F_o^2) + (0.0544P)^2 + 17.7237P]$; For **16**: $w = 1/[\sigma^2(F_o^2) + (0.0208P)^2 + 7.9834P]$; For **17**: $w = 1/[\sigma^2(F_o^2) + (0.0313P)^2 + 10.3036P]$, where $P = (F_o^2 + 2F_c^2)/3$.

**Table S2.** Selected geometric parameters (Å, º) for complexes **15**-**17**.

| Atom labels | 15 (Ln=$Nd^{3+}$) | 16 (Ln=$Eu^{3+}$) | Atom labels | 17 |
|---|---|---|---|---|
| Ln1—O1 | 2.351 (3) | 2.315 (2) | Tb1—O3 | 2.273 (2) |
| Ln1—O4* | 2.482 (5) | 2.459 (5) | Tb1—O6 | 2.271 (2) |
| Ln1—O5* | 2.450 (3) | 2.412 (5) | Tb1—O7 | 2.394 (2) |
| Ln1—O6 | 2.420 (4) | 2.395 (3) | Tb1—O8 | 2.381 (2) |
| P1—O1 | 1.503 (3) | 1.505 (2) | Tb1—O9 | 2.357 (2) |
| N1—O2 | 1.291 (6) | 1.290 (3) | Tb1—O10 | 2.441 (2) |
| N3—O3 | 1.292 (6) | 1.287 (4) | Tb1—O11 | 2.365 (2) |
| P1—O1—Ln1 | 156.4(2) | 155.84 (14) | P1—O3 | 1.493 (2) |
| | | | P2—O6 | 1.486 (2) |
| | | | N1—O1 | 1.289 (3) |
| | | | N2—O2 | 1.287 (4) |
| | | | N5—O4* | 1.305 (12) |
| | | | N6—O5 | 1.288 (3) |
| | | | P1—O3—Tb1 | 162.07 (13) |
| | | | P2—O6—Tb1 | 165.31 (15) |
| Hydrogen-bond geometry (**15**) | | | | |
| **D—H···A** | **D—H** | **H···A** | **D···A** | **D—H···A** |
| N2—H2···O4A | 0.86(3) | 2.28(6) | 3.041 (18) | 148 (8) |
| N2—H2···O4B | 0.86(3) | 2.30(7) | 3.08 (5) | 150 (8) |
| N4—H4···$O2^{i}$ | 0.83(8) | 2.16(8) | 2.939 (7) | 157 (7) |
| Hydrogen-bond geometry (**16**) | | | | |
| N2—H2···O4 | 0.86 (1) | 2.21 (3) | 2.994(12) | 151 (5) |
| N2—H2···O4A | 0.86 (1) | 2.32 (4) | 3.08(3) | 147 (5) |
| N4—H4···$O2^{i}$ | 0.86 (1) | 2.11 (2) | 2.945 (4) | 163 (3) |
| Hydrogen-bond geometry (**17**) | | | | |
| N4—H4···$O5^{i}$ | 0.85(2) | 2.11 (2) | 2.912 (3) | 158 (3) |
| N8—H8···$O2^{ii}$ | 0.85(2) | 2.01 (2) | 2.794 (4) | 153 (4) |

*For **15** and **16:** *Value correspond to average bond length, as the hfac oxygen atoms are disordered over two positions. Symmetry codes for **15** and **16**: (i) −*x*+1/2, *y*, *z*−1/2; for **17**: (i) x+1/2, −y+1/2, z−1/2; (ii) x+1/2, −y+1/2, z+1/2.

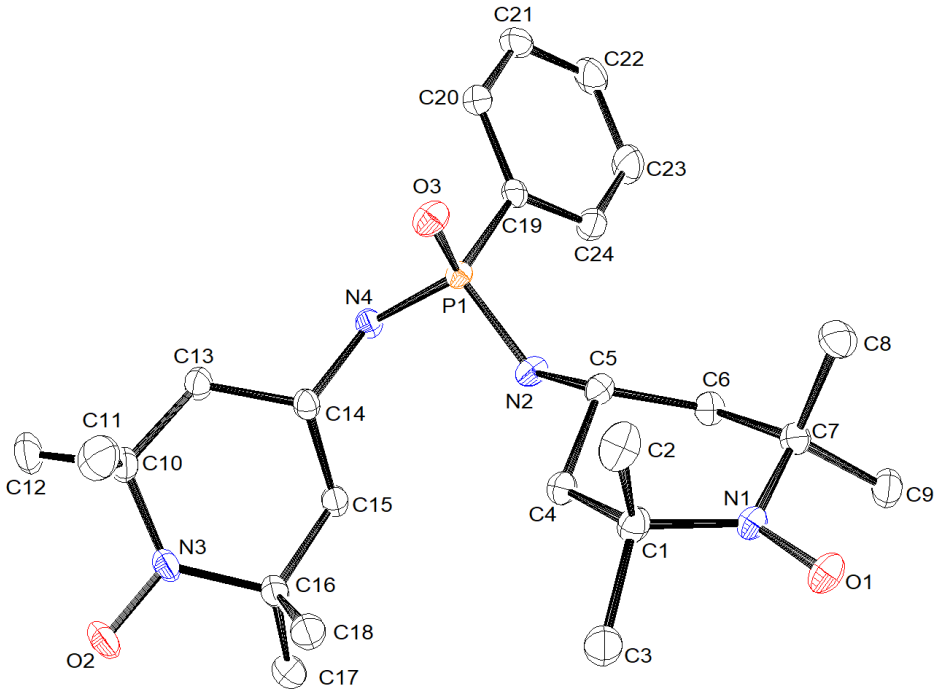


**Fig. S14**. ORTEP representation of the asymmetric unit of **13** including numbering (ellipsoids shown at 50% probability). Hydrogen atoms have been omitted for clarity.

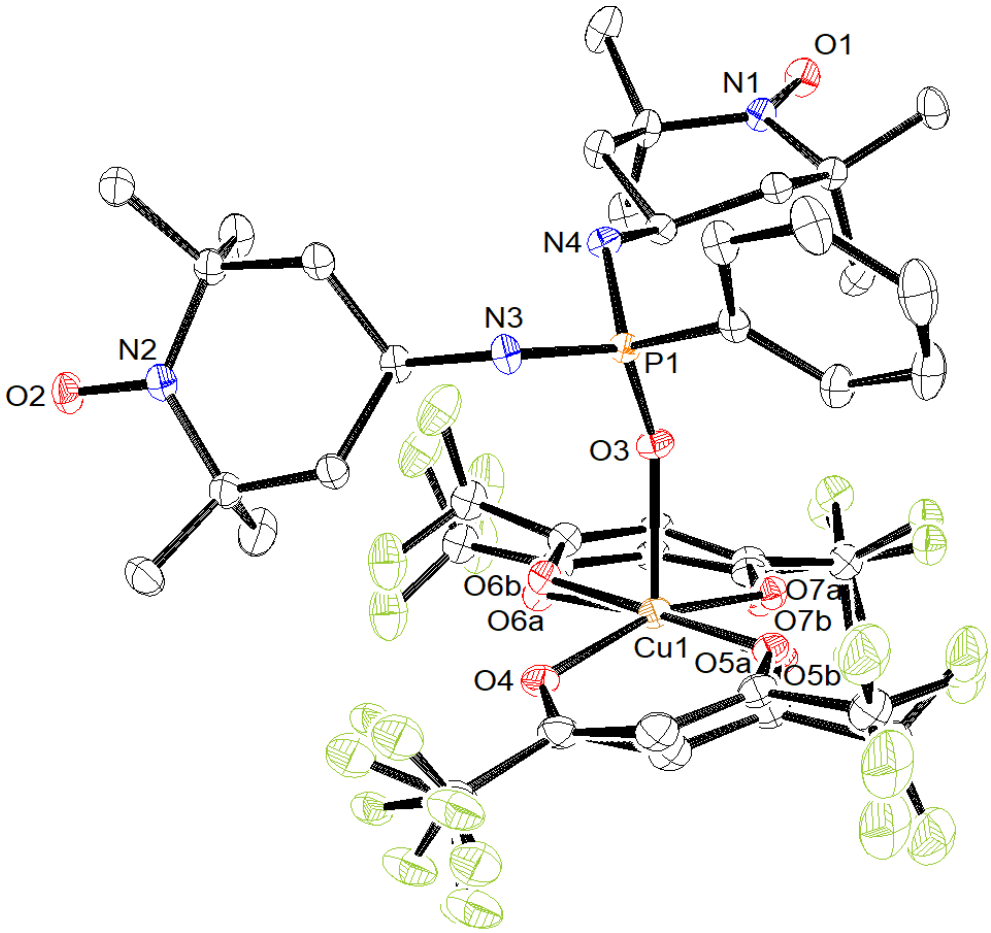


**Fig. S15**. ORTEP representation of the asymmetric unit of **14** including main atom labels (ellipsoids shown at 30% probability). Hydrogen atoms have been omitted for clarity.

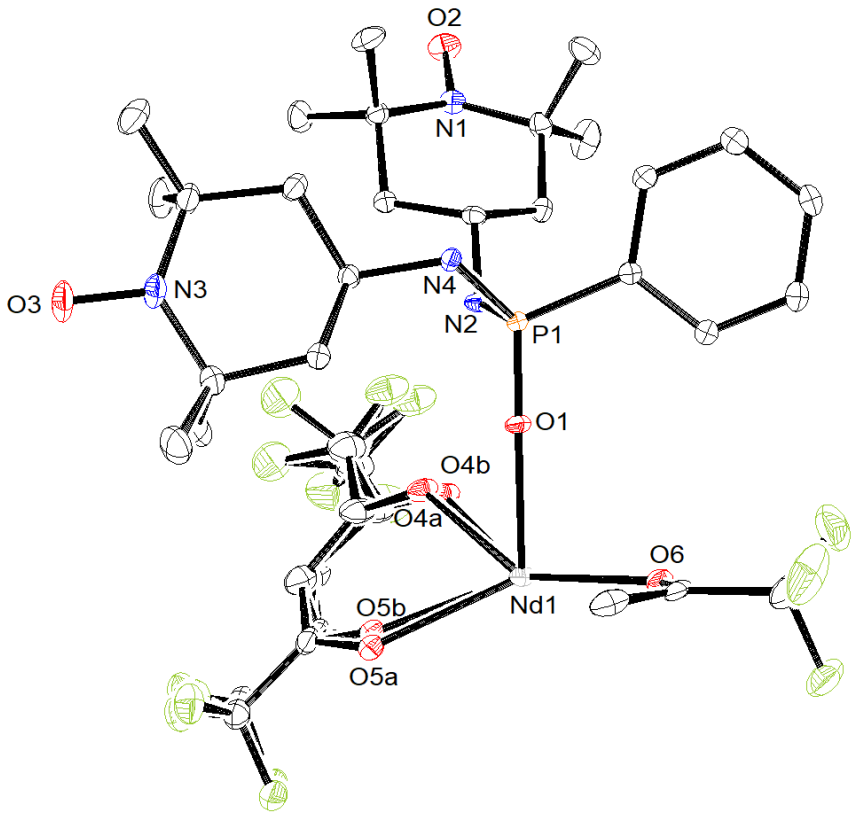


**Fig. S16.** ORTEP representation of the asymmetric unit of **15** including main atom labels (ellipsoids shown at 30% probability). Hydrogen atoms have been omitted for clarity.

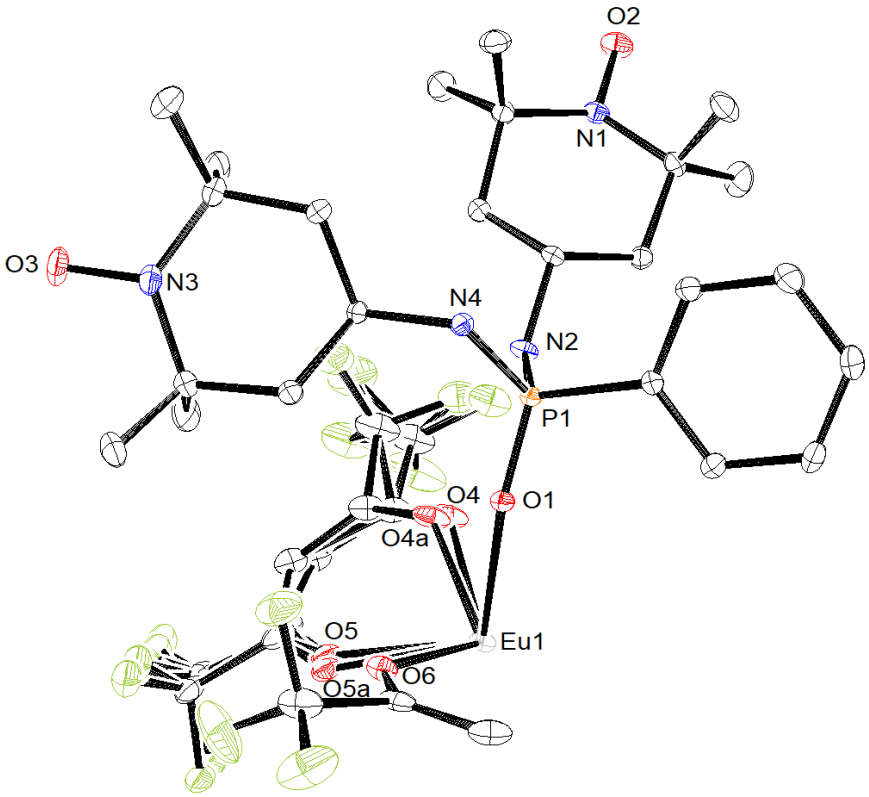


**Fig. S17**. ORTEP representation of the asymmetric unit of **16** including main atom labels (ellipsoids shown at 30% probability). Hydrogen atoms have been omitted for clarity.

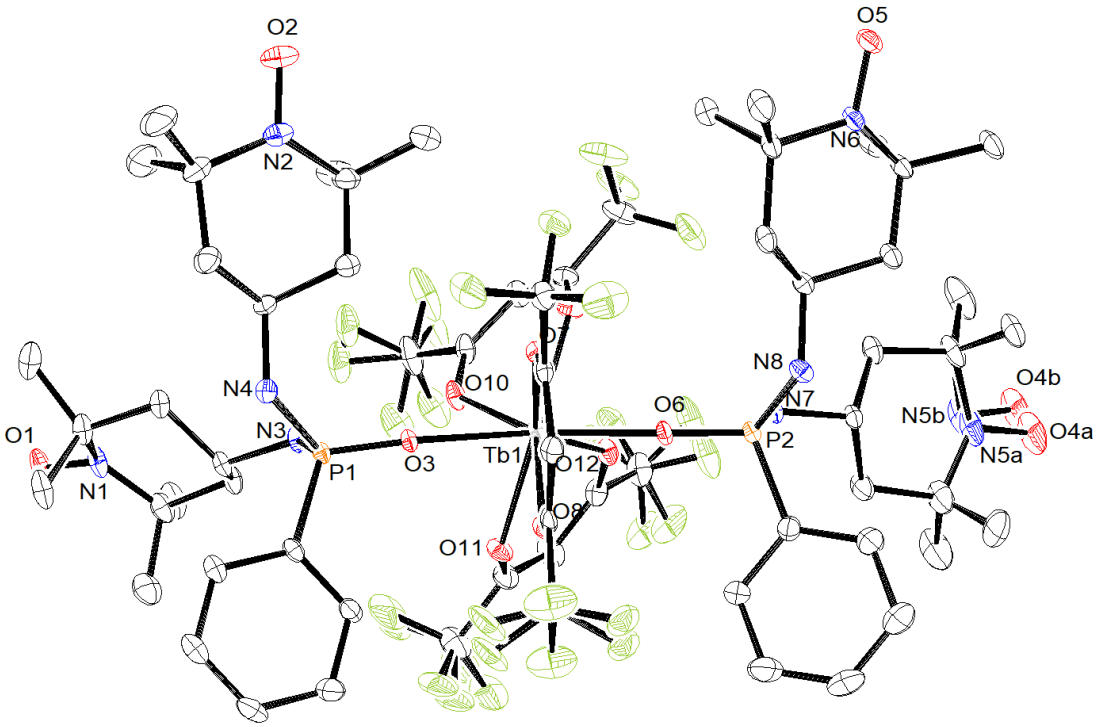


**Fig. S18**. ORTEP representation of the asymmetric unit of **17** including main atom labels (ellipsoids shown at 30% probability). Hydrogen atoms have been omitted for clarity.

**Natural Bond Orbital (NBO) Analysis Data**

**Table S3**. Natural charges ($q_{NBO}$) and spin densities ($\rho_{spin}$) of key donor sites (ωB97M-V/def2-TZVP; NBO natural populations).

| Ligand | Donor site | Atom(s) (QM numbering) | $Q_{NBO}$ (avg) | $\rho_{spin}$ (avg) |
|---|---|---|---|---|
| **1** | Nitroxide O | O1, O2 | −0.423 | 0.523 |
| **1** | Nitroxide N (radical) | N3, N6 | +0.034 | 0.448 |
| **1** | Bridging amine N (NH) | N4, N5 | −0.600 | ~0.000 |
| **5** | Piperazine N | N2, N5 | −0.445 | 0.00024 |
| **5** | Nitroxide N (radical) | N11, N16 | +0.031 | 0.446 |
| **5** | Nitroxide O | O19, O20 | −0.421 | 0.519 |
| **6** | P=O oxygen | O9 | −1.086 | ~0.000 |
| **6** | Amide N (P–NH–TEMPO) | N7 | −0.991 | ~0.000 |
| **6** | Nitroxide O | O16 | −0.418 | 0.527 |
| **6** | Nitroxide N (radical) | N4 | +0.037 | 0.443 |
| **13** | P=O oxygen | O2 | −1.112 | ~0.000 |
| **13** | Amide N (P–NH–TEMPO) | N5, N6 | −1.007 | ~0.000 |
| **13** | Nitroxide O | O3, O4 | −0.415 | 0.531 |
| **13** | Nitroxide N (radical) | N7, N8 | +0.029 | 0.442 |

**Table S4**. Selected second-order donor–acceptor stabilization energies E(2) (kcal·mol$^{-1}$) for key donor sites (NBO 7.0; ωB97M-V/def2-TZVP; only representative largest E(2) values are listed).
(a) Phosphoryl oxygen (P=O)

| Ligand | Donor (L) → Acceptor (NL) | E(2) |
|---|---|---|
| **6** | LP(3) O9 → BD*(N7–P8) | 18.22 |
| **6** | LP(2) O9 → BD*(P8–C11) | 15.25 |
| **6** | LP(2) O9 → BD*(P8–C10) | 9.26 |
| **13** | LP(3) O2 → BD*(P1–N5) | 17.49 |
| **13** | LP(2) O2 → BD*(P1–N6) | 8.33 |
| **13** | LP(2) O2 → BD*(P1–C9) | 14.97 |

(b) Piperazine nitrogens

| Ligand | Donor (L) → Acceptor (NL) | E(2) |
|---|---|---|
| **5** | LP(1) N2 → BD*(C1–C3) | 14.22 |
| **5** | LP(1) N2 → BD*(C1–N5) | 13.77 |

(c) Nitroxide oxygens

| Ligand | Nitroxide O | Donor (L) → Acceptor (NL) | E(2) |
|---|---|---|---|
| **1** | O1/O2 | LP(3) O2 → BD*(N6–C18) | 7.92 |
| **5** | O19/O20 | LP(3) O19 → BD*(N11–C13) | 6.85 |
| **5** | O19/O20 | LP(2) O19 → BD*(N11–C14) | 5.12 |
| **6** | O16 | LP(3) O16 → BD*(C3–N4) | 7.30 |
| **13** | O3/O4 | LP(3) O3 → BD*(N7–C30) | 7.00 |
| **13** | O3/O4 | LP(3) O4 → BD*(N8–C24) | 6.86 |

(d) Amide nitrogens (P–NH–TEMPO)

| Ligand | Donor (L) → Acceptor (NL) | E(2) |
|---|---|---|
| **6** | LP(1) N7 → BD*(P8–C11) | 6.29 |
| **6** | LP(1) N7 → BD*(P8–C10) | 5.87 |
| **13** | LP(1) N6 → BD*(P1–C9) | 9.01 |
| **13** | LP(1) N5 → BD*(P1–C9) | 8.57 |

**Table S5**. Local NLMO steric-exchange energies (kcal·mol$^{-1}$) for ligand **5**
(NBO/NLMO steric analysis; ωB97M-V/def2-TZVP; spin-averaged dE(i) per NLMO).

| Site | Atom(s) | Local steric cost |
|---|---|---|
| Piperazine N | N2, N5 | 84.5 |
| Nitroxide N (radical) | N11, N16 | 37.6 |
| Nitroxide O | O19, O20 | 38.8 |

**Table S6**. Global NLMO steric-exchange energies (kcal·mol$^{-1}$)
(NBO/NLMO steric analysis; ωB97M-V/def2-TZVP).

| Ligand | Total steric exchange (α) | Total steric exchange (β) | Overall spin-averaged total | Overall disjoint steric exchange |
|---|---|---|---|---|
| **1** | 844.45 | 784.58 | 1629.03 | 875.61 |
| **5** | 958.66 | 898.24 | 1856.90 | 991.35 |
| **6** | 888.58 | 858.48 | 1747.06 | 762.06 |
| **13** | 1046.54 | 988.24 | 2034.78 | 993.07 |

**References**

1 (*a*) M. Andruh, E. Bakalbassis, O. Kahn, J. C. Trombe and P. Porchers, *Inorg. Chem.,* 1993, **32**, 1616; (*b*) O. Kahn, *Molecular Magnetism*, VCH Publishers, Inc., New York, 1993.